Cappadonia, Chiara, Coco, Laura, Buccolini, Marcello, Rotigliano, Edoardo (2016). From Slope Morphometry to Morphogenetic Processes: An Integrated Approach of Field Survey, Geographic Information System Morphometric Analysis and Statistics in Italian Badlands. LAND DEGRADATION & DEVELOPMENT, vol. 27, p. 851-862, ISSN: 1085-3278, doi: 10.1002/ldr.2449

From Slope Morphometry to Morphogenetic Processes: An Integrated Approach of Field Survey, Geographic Information System Morphometric Analysis and Statistics in Italian Badlands

Chiara Cappadonia,Laura Coco,Marcello Buccolini,Edoardo Rotigliano

Abstract

Calanchi (singular: calanco) represent a typical example of badlands in the Italian peninsula, which rapidly evolve on clayey terrains such as the widespread Pliocene–Pleistocene marine clays. The present study aimed at investigating the role of the slope morphometry on the typology and distribution of morphogenetic processes in a calanchi area located in southern Italy. The research included detailed geomorphological surveying as well as morphometric and statistical analyses. The study area was first subdivided into individual hydrographic units (HUs), for which field survey allowed to identify the dominant denudation processes, their intensity and the distribution of the associated landforms (pipes, rills, gullies and landslides). The morphometry of each HU was characterised by calculating the morphometric slope index (*MSI*) on a reconstructed digital elevation model. By statistically comparing the morphogenetic and morphometric data, the influence of the slope morphometry on the type, distribution and evolution of the calanchi erosion process has been highlighted. In particular, through a cluster analysis, the groups of HUs having similar dominant processes were identified, and by applying the analysis of variance, the effect of the *MSI* on the identified clusters was analysed. Two clusters were identified, which revealed the relative importance of morphogenetic processes and the strict connection between surface and subsurface landforms. These two clusters were discriminated by the *MSI* value (high *MSI* favoured mass movements, while low *MSI* favoured gully erosion and piping), highlighting the importance of slope morphometry in driving the morphogenetic hillslope processes.

Introduction

Badlands are considered as ‘ideal field laboratories’ for studying landscape evolution because they are like miniature fluvial systems in both the spatial and temporal scales, where it is possible to directly observe at the slope scale the interconnections between hillslope processes and landforms (Schumm, 1956; Bryan & Yair, 1982; Howard, 1994; Campbell, 1997; Alexander *et al*., 2008; Dickie & Parsons, 2012; Yair *et al*., 2013). In badland areas, where the changes of the landforms occur faster than in other types of landscapes, it is possible to measure the erosion rates and to evaluate the spatial and time evolution of landforms within a short time interval just like in a laboratory (Howard, 1994; Gallart *et al*., 2013). Besides, badlands and abandoned fields are two of the more sensitive ecological systems for studying the interactions between soil erosion and plant establishment in the Mediterranean (Cerdà & García-Fayos, 1997). Badlands allow to understand (Solé *et al*., 1997; Cerdà, 1999) the role of the hydrological and morphological factors in controlling soil erosion and soil quality deterioration (Gabarrón-Galeote *et al*., 2013; Zhao *et al*., 2013; Erkossa *et al*., 2015; Seutloali & Beckedahl, 2015). In this sense, the studies about badlands allow to define plan restoration and rehabilitation strategies in areas of high soil and water losses (Cerdà *et al*., 2009; Lee *et al*., 2013; Mekonnen *et al*., 2015, 2015). Badlands are defined as deeply dissected landscape with high drainage density and short steep slopes with sparse or absent vegetation, which typically shape erodible terrains, in regions dominated by overland flow erosion (Bryan & Yair, 1982; Howard, 1994). Their morphodynamic evolution is influenced by numerous factors including as follows: (i) lithology and soil properties (Faulkner *et al*., 2000; Battaglia *et al*., 2003; Farifteh & Soeters, 2006; Kasanin-Grubin, 2013); (ii) climate (Torri & Bryan, 1997; Kuhn & Yair, 2004; Regüés & Gallart, 2004; Clarke & Rendell, 2010); (iii) topographic features (Cerdà & García-Fayos, 1997; Calzolari & Ungaro, 1998; Clarke & Rendell, 2006; Nadal-Romero *et al*., 2007; Buccolini & Coco, 2010, 2013; Buccolini *et al*., 2012; Caraballo-Arias *et al*., 2014, 2015); (iv) vegetation cover (Cerdà & García-Fayos, 1997; Guàrdia *et al*., 2000; Nadal-Romero *et al*., 2014); and (v) human impact (Clarke & Rendell, 2000; Buccolini *et al*., 2007; Capolongo *et al*., 2008; Castaldi & Chiocchini, 2012; Torri *et al*., 2013; Vergari *et al*., 2013). The badland landscapes are affected by the interplay among several hydro-morphological phenomena like weathering, Hortonian runoff, mass movements, piping and hillslope–channel coupling, involving interactions between slope processes and basal stream or gully activity (Schumm, 1956; Faulkner *et al*., 2008; Desir & Marín, 2013). However, the shaping of badlands is due to both surface (water erosion) and subsurface processes (Alexander, 1980; Gutierrez *et al*., 1997; Cerdà, 1999; Clarke & Rendell, 2006; Della Seta *et al*., 2009), such as mass movements and piping. In particular, depending on the site conditions (e.g. bedrock lithology, presence, thickness, hydrological and mineralogical soil properties), the piping processes can play an important role in the development and deepening of gullies, for example, through the collapse of the pipes' roofs (Cappadonia *et al*., 2011; Buccolini *et al*., 2012; Pulice *et al*., 2012). Pipes are generally located either between the weathered surface layer and the bedrock or along the fractures or between layers of different hardness and permeability (Farifteh & Soeters, 1999; Romero Díaz *et al*., 2007). The mass movements are mainly flow-type shallow landslides (Alexander, 1980; Moretti & Rodolfi, 2000; Farifteh & Soeters, 2006), which generally affect the gullies (Pulice *et al*., 2012).

The erosion rates on the badlands slopes have been widely estimated through discrete observations of topographic changes measured by means of erosion pins or profile metres (Sirvent *et al*., 1997; Clarke & Rendell, 2006; Della Seta *et al*., 2007; Ciccacci *et al*., 2008; Cappadonia *et al*., 2011), topographic and geographic information system (GIS) analysis (Buccolini & Coco, 2010, 2013; Buccolini *et al*., 2012; Caraballo-Arias *et al*., 2014, 2015), rainfall simulation experiments (Bouma & Imeson, 2000; Martínez-Murillo *et al*., 2013), digital photogrammetric methodologies (Aucelli *et al*., 2014) or terrestrial laser scanning surveys (Vericat *et al*., 2014). Other studies were based on field observation and laboratory experiments (Farifteh & Soeters, 2006; Pulice *et al*., 2012; Martínez-Murillo *et al*., 2013; Buccolini *et al*., 2014). All these studies demonstrated that badland areas are affected by high and rapid erosion rates.

Italian badlands mainly consist of two landforms, which are typically incised into Pliocene–Pleistocene marine clays: biancane and calanchi (Vittorini, 1977; Alexander, 1982). Biancane (singular: biancana) are small clayey domes that reach a height of about 10 m, with a sub-horizontal basal pediment (Calzolari & Ungaro, 1998; Clarke & Rendell, 2006; Torri *et al*., 2013). These are typically located near the foot of the slopes or at the hill summit and are generally associated to gently dipping slopes (Torri & Bryan, 1997; Phillips, 1998; Della Seta *et al*., 2007). Calanchi, which are the focus of this research, can be considered as miniature drainage systems whose rapid evolution is controlled by mineralogical and particle size characteristics of the involved lithotypes, the structural and morphometric features of the slopes and the climatic regime of the areas. The steep clayey calanchi slopes are characterised by a dense alternation of narrow furrows and sharp ridges, varying in height from few metres to several decametres (Alexander, 1980; Clarke & Rendell, 2000; Moretti & Rodolfi, 2000). Two typologies of calanchi can be distinguished with regard to their drainage network patterns (Buccolini & Coco, 2010): dendritic and parallel. The former typology has one main furrow that is tributary to the external drainage network and is similar to a miniature basin also in its evolution (Howard, 1994, 1997), while the latter has several parallel furrows and evolves through the parallel retreat of the slope (Della Seta *et al*., 2007). Alexander (1980) highlighted that calanchi and biancane develop mainly on terrains rich in clay, being generally associated with landslides.

As calanchi are similar to miniature river basins, they can be studied using the morphometric analysis, which is typically applied to the fluvial systems (Howard, 1997). There are various studies focused on quantitative geomorphic analysis aimed at assessing the influence of slope morphometry on the drainage network (Parker, 1977; Schumm et al., 1987; Montgomery & Dietrich, 1994; Oguchi, 1997; Tucker & Bras, 1998; Talling & Sowter, 1999; Montgomery, 2001; Pelletier, 2003; Lin & Oguchi, 2004). In particular, our recent researches focused on the application of drainage basins analysis to the study of the hydrographic units (HUs) in which calanchi areas can be subdivided (Buccolini & Coco, 2010, 2013; Buccolini et al., 2012). Based on these studies, the following main outcomes were achieved:

- Calanchi inception occurs not only on steep slopes but also on gentle (9–30°) ones (Buccolini & Coco, 2010).
- The introduction of morphometric slope index (*MSI)* demonstrated its validity as a possible unique reference morphometric index for describing the overall features of the slopes, by combining their size (three-dimensional and two-dimensional area, A_{3D} and A_{2D}), length (L), shape (as circularity ratio, R_c; Miller, 1953), gradient (which affects the ratio A_{3D}/A_{2D}) and width (in terms of $L \times R_C$) through the formula (Buccolini *et al*., 2012; Buccolini & Coco, 2013):

$$MSI = \frac{A_{3D}}{A_{2D}} \times L \times R_c \quad (1)$$

- *MSI* controls calanchi presence and characteristics, allowing to predict the structure of hydrographic networks and to quantify the rate of soil erosion (Buccolini *et al*., 2012).
- For three sample areas in central Italy, the inception of erosion processes, both linear and areal, is correlated to the *MSI* value (Buccolini & Coco, 2013).

The present paper introduces a further in-depth analysis of the use of *MSI* and aims at understanding the role of the calanchi slope morphometry in controlling the typologies of the dominant morphogenetic processes and their connected landforms, by means of detailed field and remote geomorphological surveys, GIS-based morphometric analysis and multivariate statistical analysis.

The study area, which is named Catalfimo, is located in northern Sicily and is enough representative of badland areas in Italy for both environmental conditions and geomorphic processes, including an extreme variety of landforms and morphogenetic processes (mainly on-slope interactions between weathering, runoff, piping and landslides). Moreover, the Catalfimo area has been monitored since many years from an interdisciplinary team and was previously studied as sample area in the framework of the Italian badlands (Buccolini *et al*., 2012; Pulice *et al*., 2012; Caraballo-Arias *et al*., 2014, 2015). Furthermore, the availability of a rich archive of topographic information and a high-resolution (2-m cell size) laser scanner-derived digital elevation model (DEM), provided by the Sicilian Regional Department for Territory and Environment, enables detailed morphometric analyses.

Materials and Methods

Geological and Geomorphological Setting

The study area is located along the Apennine chain area in the central segment of the Sicilian–Maghrebian fold-and-thrust belt (Figure 1a), Early–Middle Miocene in age (Catalano *et al*., 2000). In particular, the Catalfimo calanchi front is a part of the Scillato basin, a narrow thrust-top syntectonic basin developed since the late Tortonian (Gugliotta & Agate, 2010; Gugliotta & Gasparo Morticelli, 2010). This sector of the Sicilian chain is characterised by four different geomorphological systems, each marked by a well-defined morphostructural style and a typical association of landforms (Agnesi *et al*., 2000, 2005):

monoclinal faulted blocks mainly producing structural landforms; faulted carbonate massive blocks affected by intensely karstified planation surfaces; intensively faulted and fractured relief, mainly affected by deep-seated gravitational slope deformation and physical weathering; and systems of clayey–sandy slopes affected by frequent surface landslides.

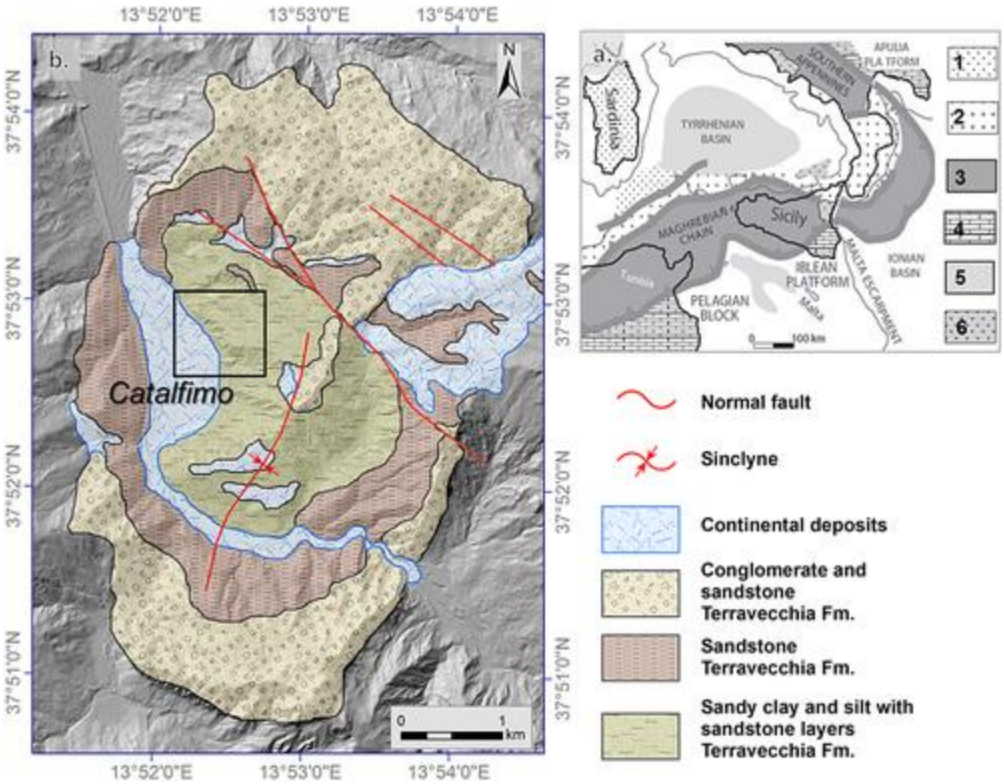

Figure 1
Geological scheme of the Scillato basin (b) and tectonic scheme of the central Mediterranean (a) modified after Catalano *et al*., 2000 (1. Corsica–Sardinia; 2. Kabilo–Calabride units; 3. Maghrebian and southern Apennines chain; 4. Foreland and mildly folded foreland; 5. Extensional areas; 6. Pliocene quaternary vulcanites). The red arrow indicates the location of the study area. This figure is available in colour online at wileyonlinelibrary.com/journal/ldr.

The Scillato basin is a synclinal structure with its major axis trending North-Southwest, being dissected by a North-Northeast–South-Southwest fault system (Catalano *et al*., 2010). It is filled by the Terravecchia formation, over 1,300 m thick, characterised by a great variability of rock types and sedimentary facies (Gugliotta, 2012) consisting of conglomerate, sandstone, silt and clay arranged in a multi-cyclic sequence from alluvial clastic to marine (Figure 1b).

The climate is meso-Mediterranean, characterised by hot dry summers and mild wet winters with bimodal rainfall distribution. Rainfall data indicate a mean annual value of about 620 mm, with a maximum in January and a minimum in July. Temperature data show an average annual temperature of 16 °C, an average maximum of 24 °C during July to August and an average minimum of 9 °C in the period from November to January. The wet season occurs from October to April and corresponds to the period of maximum intensity of the erosion processes (Cappadonia *et al*., 2011).

The landscape of the Scillato basin is characterised by a high variability of erosion landforms and processes (Figure 2a–f), strongly influenced by the structural setting of a cuesta relief (Figure 2a) located at the centre of the area. Sheet wash, creep and solifluction, with rare gullies and landslides, mainly affect the low-angle N-facing slopes. Conversely, rill and gully erosion, piping (Cappadonia *et al*., 2011) and mass movements (shallow slide/flow and fall) widely affected the steep S-facing scarp slopes and create a typical calanchi front, which is arranged in a sub-parallel naturally evolving pattern.

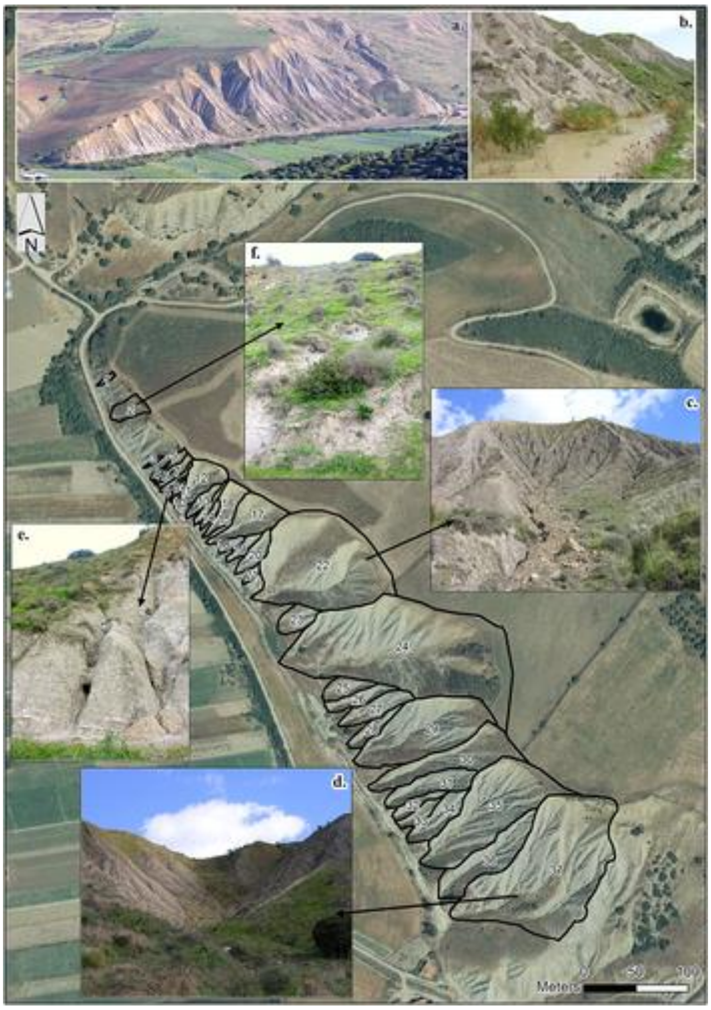

Figure 2
The Catalfimo area subdivided into 37 hydrological units. The boxes show the panoramic views of the calanchi (a and b) and some details of the hydrographic units: a flow-type landslide affecting the main channel (c); landslides on the right hydrographical side (d); gullies, rills and pipes (e); and shallow landslides in the upstream sector (f). This figure is available in colour online at wileyonlinelibrary.com/journal/ldr.

The calanchi area at Catalfimo develops on slopes constituted by an alternation of silty clay and clayey silt layers, with a 2-m thick sandstone cape rock, which is affected by falls whose debris tends to be channelled in the underlying gullies. The main processes within the study area are piping and gullying (the latter often created because of the pipes roof's collapse) and surficial landslides that shape rounded valleys and divides. Pipes (Figure 2e) develop at different depths with length and diameter varying from few millimetres to some decimetres: micro, small and moderate pipes *sensu* Farifteh & Soeters (1999). These landforms are located along the whole front and are closely related to a weathered hardwearing surface horizon coupled with the opening of desiccation cracks and the decay of roots.

The clayey portions underlying the cape rock have the typical calanchi features (Figure 2a and b): high roughness due to weathering processes, presence of micro-reliefs under more resistant elements (shells, leaves and pebbles) due to the action of the heavy rain, surface whitish salt efflorescence during the spring and reddish weathered bands throughout the year (Pulice *et al*., 2012). The substrate materials are relatively coarse grained, in which silt dominates over the clay, with scarce sand fraction. The coarse (sand and silt) fraction has quite homogeneous mineralogy, with quartz always dominating over calcite and feldspars, followed by dolomite and very poor phyllosilicates. Besides, the fine fraction has an overall homogeneity: the clay minerals consist of illite, kaolinite, smectite and traces of chlorite. Geotechnical analysis indicated that the materials can be classified as cohesive and consists in inorganic silt with intermediate compressibility and inactive clays (Pulice *et al*., 2012).

Methodology

The main objective of this research was to exploit statistical analysis tools to study the influence of the general slope morphometry (summarised by *MSI*) on the presence and distribution of morphogenetic processes. For this purpose, the Catalfimo calanchi front was first partitioned into HUs, for each of which a detailed field survey and a morphometric analysis were carried out. In a second stage, by using the cluster analysis, the morphodynamic characteristics of each HU was assessed as an expression of the recognised multiple morphogenetic processes, and the relation between surface and subsurface landforms was pointed out. Finally, the potential discriminating effect of *MSI* on the identified clusters was investigated by applying the analysis of variance (ANOVA).

On the basis of field and GIS-based analysis, the Catalfimo area (Figure 2) was subdivided into 37 HUs: each unit is directly connected to the external drainage network (Figure 2b), corresponding to a single gully tributary and including the surrounding calanco unit and upslope area (Buccolini & Coco, 2010; Buccolini *et al*., 2012). Each HU was characterised in terms of morphogenetic process and related landforms, based on a detailed field and remote geomorphological survey. In particular, once a review of the existing geomorphological data and an aerophotogrammetric investigation were completed, a field recognition was carried out during the winter time (February 2012), which is the period when typically runoff-related slope processes have their maximum intensity in northern Sicily.

A special survey form was prepared to rationalise the field activity. For each HU, the presence and/or prevalence of the different slope processes, estimated from the recognised landforms, was assessed. For this purpose, each hydrological unit was subdivided into three sub-sectors (upstream, central and bottom), and based on an expert geomorphological analysis, the presence and the predominance of the different types of landforms were estimated in an ordinal scale. For the piping process, the identification was limited to presence/absence recognition; in fact, for the pipes, it was only possible to identify the outlet of the water flow but not the complete underground system. Their spatial density was evaluated in high, medium and low. However, collapsed/not collapsed pipes were distinguished, and in light of their size, micro, small and moderate to large pipes were classified, according to Farifteh & Soeters (1999). The diameter of the pipes was measured by using a sliding calliper and a metro, while their length was taken along the collapsed roofs channels, after having checked their continuity by using a tracer solution. For rills, the presence or absence was only indicated as these ephemeral landforms have a poor morphological impact on the slopes, because of their rapid evolution and seasonal modification. Dendritic and parallel rills drainage systems were distinguished, and their spatial density was evaluated in high, medium and low. For gullies and landslides, presence/absence and prevalence with respect to the other landforms were indicated. As regards the prevalence, gullies were considered to prevail on landslides when they were very carved and only small landslides occurred on the lateral slopes, without interesting the main channel. On the contrary, when the landslide debris filled or rounded the channel or when the landslides affected wide portions of the crests or lateral slopes, landslides were considered as prevalent. For gullies, the number (one or more than one), the depth (deep or shallow) and the interaction with the main channel (carved or not carved) were evaluated. For landslides, the size (small, medium or large), the depth (shallow or very shallow) and the interaction with the main channel (filled or not filled) were evaluated.

Once the morphodynamic characteristics of the HUs were defined, a DEM analysis was carried out to derive their current and pre-erosion morphometric features. By means of ArcGIS 9·3 (ESRI, Redlands, CA, USA) hydrological tools, straight contour lines connecting the points with the same heights on the opposite sides of each HU watershed divide (Buccolini *et al*., 2012) (Figure 3a) were drawn, so that a pre-incision 2-m cell DEM was then obtained, by using the *Topo-to-Raster* interpolation tool (Hutchinson, 1989), starting from these new contour lines. This pre-incision DEM was taken as undisturbed from the calanchi erosion and considered as reflecting the pre-erosion topography. In doing this, the heights of the water divides of each HU border were considered as constant, according to the parallel slope retreat evolution, which typically affects the calanchi fronts

(Della Seta *et al*., 2007). Exploiting both the pre-incision and the current DEMs, reconstructed (Figure 3b) three-dimensional surface area (A_r), plan area (A_{2D}), circularity ratio (R_c; Miller, 1953) and slope length (L) were calculated and used to obtain *MSI* values via Equation 1. By means of statistics, morphometric and morphogenetic data were then compared in order to analyse the characteristics of the morphogenetic processes in the calanchi HUs. A two-step cluster analysis on the erosion data was performed, using SPSS Statistics Desktop V22·0—trial packages (IBM, Armonk, NY, USA), in order to identify the groups of HUs having similar morphodynamic conditions, by minimising the within-cluster variance and maximising the between-cluster variance of the data. This algorithm is capable of handling both continuous and categorical variables and is based on a two-stage approach: in the first step, it groups the records into many small sub-clusters by estimating the Euclidean distance between pairs of objects; then, it groups the sub-clusters into the proper number of clusters, automatically determined on the basis of statistical evaluation criteria. The first step is repeated through an iterative procedure until the cluster centre position remains stable with respect to the initial situation. Furthermore, the procedure indicates each variable's importance for the construction of a specific cluster, allowing the interpreter to investigate the geomorphological meaning of the model.

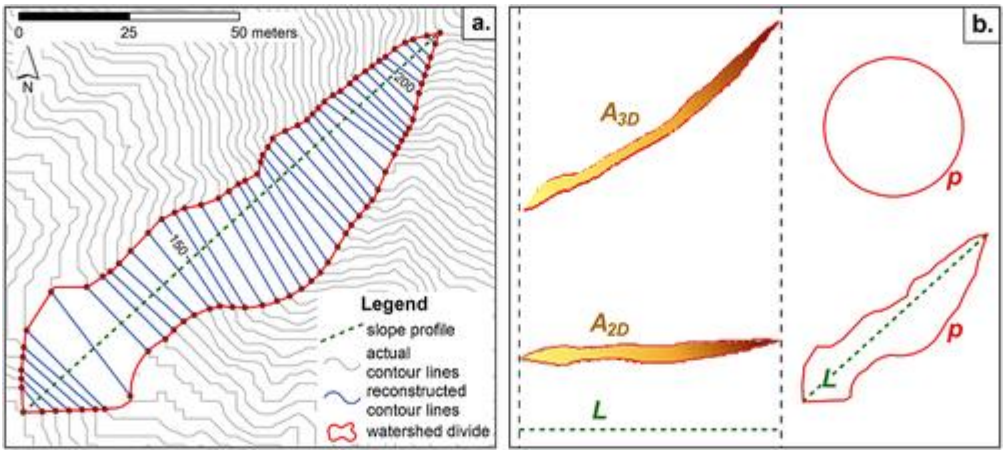

Figure 3
Example of pre-erosion topography reconstruction (a) and parameters used for calculating morphometric slope index (b): A_{2D} = plane area, A_r = reconstructed surface area, L = plane length and p = drainage basin perimeter and circle circumference (equal to basin perimeter). Contour interval is 2 m. This figure is available in colour online at wileyonlinelibrary.com/journal/ldr.

Once the clusters of erosion processes were identified, the ANOVA (one-way ANOVA) was performed for investigating the effect of the slope morphometry on the identified groups of processes, using *MSI*. The clusters were considered as predictors (1 and 2), and *MSI* was considered as dependent variable.

Results

The geomorphological field survey showed that the most widespread landforms in the study area are produced by the action of surface waters (e.g. rill and gully erosion, infiltration along mud cracks, accumulation of mud or debris), sub-surficial waters (piping) and slope deformations (falls, slides and flows). Gullies generally corresponded to the principal HU channels that resulted very incised and surrounded by sharp ridges. Landslides were generally very shallow and affected the lateral slopes of the HUs, determining a more rounded morphology and often filling the channels. Besides, a different spatial distribution and intensity of the mapped landforms and related processes, from NW to SE, arose.

The whole data set describing the slope processes acting on the HUs is reported in Figure 4, which shows some examples of the landforms recognised in the HUs together with the complete geomorphological field data. The HUs in which landslides prevailed (e.g. HU37 and HU30) were characterised by the presence of rounded crests, and their main channels were filled by eroded material with rill and gully erosion frequently affecting their lower sectors. The HUs in which runoff prevails showed sharper ridges and more carved channels; generally, the main channel developed as a large gully, while rills were present as an ephemeral system on the lateral slopes (e.g. HU6, HU27, HU35 and HU47). In these HUs, some small dome reliefs could be observed where the rills created a typical centrifugal drainage. On the other hand, the material of the small shallow flow-type landslides that affected the lateral slopes (e.g. HU29) often filled the bigger gullies. The HUs in which piping erosion developed (e.g. HU4, HU10, HU21 and HU28) were mainly located in the north-western part of the calanchi front. The cross section of pipes varied from few millimetres to 30 cm in diameter and from few centimetres to some metres in length.

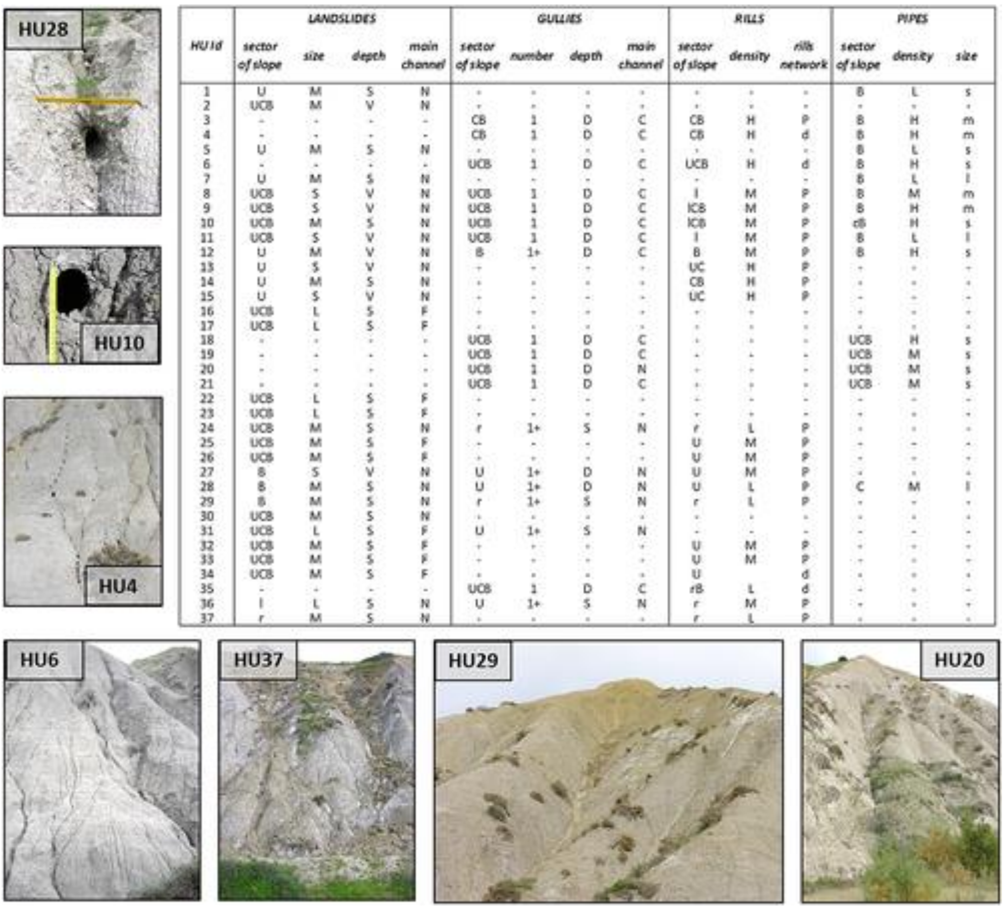

HU Id	LANDSLIDES				GULLIES				RILLS			PIPES		
	sector of slope	size	depth	main channel	sector of slope	number	depth	main channel	sector of slope	density	rills network	sector of slope	density	size
1	U	M	S	N	-	-	-	-	-	-	-	B	L	s
2	UCB	M	V	N	-	-	-	-	-	-	-	-	-	-
3	-	-	-	-	CB	1	D	C	CB	H	p	B	H	m
4	-	-	-	-	CB	1	D	C	CB	H	d	B	H	m
5	U	M	S	N	-	-	-	-	-	-	-	B	L	s
6	-	-	-	-	UCB	1	D	C	UCB	H	d	B	H	s
7	U	M	S	N	-	-	-	-	-	-	-	B	L	l
8	UCB	S	V	N	UCB	1	D	C	I	M	p	B	M	m
9	UCB	S	V	N	UCB	1	D	C	ICB	M	p	B	H	m
10	UCB	M	S	N	UCB	1	D	C	ICB	M	p	cB	H	s
11	UCB	S	V	N	UCB	1	D	C	I	M	p	B	L	l
12	U	M	V	N	B	1+	D	C	B	M	p	B	H	s
13	U	S	V	N	-	-	-	-	UC	H	p	-	-	-
14	U	M	S	N	-	-	-	-	CB	H	p	-	-	-
15	U	S	V	N	-	-	-	-	UC	H	p	-	-	-
16	UCB	L	S	F	-	-	-	-	-	-	-	-	-	-
17	UCB	L	S	F	-	-	-	-	-	-	-	-	-	-
18	-	-	-	-	UCB	1	D	C	-	-	-	UCB	H	s
19	-	-	-	-	UCB	1	D	C	-	-	-	UCB	M	s
20	-	-	-	-	UCB	1	D	N	-	-	-	UCB	M	s
21	-	-	-	-	UCB	1	D	C	-	-	-	UCB	M	s
22	UCB	L	S	F	-	-	-	-	-	-	-	-	-	-
23	UCB	L	S	F	-	-	-	-	-	-	-	-	-	-
24	UCB	M	S	N	r	1+	S	N	r	L	p	-	-	-
25	UCB	M	S	F	-	-	-	-	U	M	p	-	-	-
26	UCB	M	S	F	-	-	-	-	U	M	p	-	-	-
27	B	S	V	N	U	1+	D	N	U	M	p	-	-	-
28	B	M	S	N	U	1+	D	N	U	L	p	C	M	l
29	B	M	S	N	r	1+	S	N	r	L	p	-	-	-
30	UCB	M	S	N	-	-	-	-	-	-	-	-	-	-
31	UCB	L	S	F	U	1+	S	N	-	-	-	-	-	-
32	UCB	M	S	F	-	-	-	-	U	M	p	-	-	-
33	UCB	M	S	F	-	-	-	-	U	M	p	-	-	-
34	UCB	M	S	F	-	-	-	-	U	-	d	-	-	-
35	-	-	-	-	UCB	1	D	C	rB	L	d	-	-	-
36	I	L	S	N	U	1+	S	N	r	M	p	-	-	-
37	r	M	S	N	-	-	-	-	r	L	p	-	-	-

Figure 4
Table summarising the hydrographic unit field survey according to the survey form, and some examples of the landforms in the hydrographic units (sector of slope: U, upstream; C, central; B, bottom. Landslides size: S, small; M, medium; L, large. Landslides depth: S, shallow; V, very shallow. Landslides main channel: F, filled; N, not filled. Gullies number: 1, one; 1+, more than one. Gullies depth: D, deep; S, shallow. Gullies main channel: C, carved; N, not carved. Rills density: H, high; M, medium; L, low. Rills network: p, parallel; d, dendritic. Pipes density: H, high; M, medium; L, low. Pipes size: m, micro; s, small; l, moderate to large). This figure is available in colour online at wileyonlinelibrary.com/journal/ldr.

The results of the morphometric analysis are presented in Table 1 together with the codes summarising the different morphogenetic processes, differentiated into categories depending on their relative importance: 0 for 'absence', 1 for 'presence' and 2 for 'prevalence'. Table 1 also indicates the two main clusters in which the HUs were grouped. In fact, the results of the cluster analysis highlighted that the 37 HUs can be grouped into two clusters (Table 2): the first contains 22 HUs, which represented 59·5% of the data, mainly characterised by the absence of gullies ($G = 0$) and pipes ($P = 0$), the prevalence of landslides ($Ls = 2$) and the presence of rills ($R = 1$); the second contains 15 HUs, which represented 40·5% of the data, mainly characterised by the gullies prevalence ($G = 2$), the presence of pipes ($P = 1$) and rills ($R = 1$) and the absence of landslides ($Ls = 0$). The absolute and relative distributions of each variable category in the two clusters are summarised in Table 3. The slope processes were aggregated in the two clusters according to their relative importance, ranging from 0 to 1, for the least and most important ones, respectively. The main discriminating factors were gullies and landslides, followed by pipes, while rills were the least important (Figure 5).

Table 1. Morphometric parameters and landforms in the hydrographic unit and the two main clusters in which the landforms can be grouped

Calanco HU	Morphometry					Landforms				Cluster
	R_C	A_{3D} (m²)	A_{2D} (m²)	*L* (m)	*MSI* (m)	*Ls*	*G*	*R*	*P*	
1	0·50	127·2	82·6	20·3	15·5	2	0	0	1	1
2	0·69	734·6	553·3	36·1	32·8	2	0	0	0	1
3	0·30	77·5	54·4	22·9	9·7	0	2	1	1	2
4	0·37	118·5	83·1	24·7	12·8	0	2	1	1	2
5	0·27	285·9	203·7	43·5	16·6	2	0	0	1	1
6	0·36	131·3	93·4	27·1	13·8	0	2	1	1	2
7	0·37	400·6	284·5	43·2	22·2	2	0	0	1	1
8	0·24	236·1	168·4	45·3	14·9	1	2	1	1	2
9	0·24	99·7	71·0	29·0	9·7	1	2	1	1	2
10	0·42	141·3	102·3	25·9	15·1	1	2	1	1	2
11	0·36	59·4	43·8	18·8	9·1	1	2	1	1	2
12	0·59	1,473·0	1,170·9	59·9	44·4	1	2	1	1	2
13	0·45	515·4	377·5	47·5	29·1	2	0	1	0	1
14	0·24	345·9	258·3	55·5	17·9	2	0	1	0	1
15	0·40	242·6	178·7	34·5	18·9	2	0	1	0	1
16	0·45	1,124·6	877·4	62·5	36·0	2	0	0	0	1
17	0·52	2,073·2	1,697·7	73·6	46·6	2	0	0	0	1
18	0·53	284·1	214·4	31·8	22·5	0	2	0	1	2
19	0·42	433·2	317·8	45·1	25·8	0	2	0	1	2
20	0·49	812·0	615·7	57·4	37·3	0	2	0	1	2
21	0·55	202·3	153·0	26·7	19·5	0	2	0	1	2
22	0·75	10,498·8	9,339·3	125·2	106·1	2	0	0	0	1
23	0·70	940·4	744·4	47·4	41·9	2	0	0	0	1
24	0·56	17,768·5	15,947·3	223·5	139·9	2	1	1	0	1
25	0·55	826·1	703·9	55·8	36·2	2	0	1	0	1
26	0·35	924·6	755·2	73·5	31·9	2	0	1	0	1
27	0·47	1,414·7	1,097·1	76·3	46·1	1	2	1	0	2
28	0·35	746·3	631·2	68·7	28·6	1	2	1	1	2
29	0·61	6,693·8	5,435·3	138·2	103·2	2	1	1	0	1
30	0·31	3,894·8	3,205·0	141·4	53·5	2	0	0	0	1
31	0·43	1,953·0	1,544·9	94·6	51·8	2	1	0	0	1
32	0·35	619·6	498·5	58·8	25·9	2	0	1	0	1
33	0·40	589·3	477·2	52·5	26·2	2	0	1	0	1
34	0·49	1,539·8	1,231·1	79·5	48·3	2	0	1	0	1
35	0·49	8,013·6	6,463·0	148·1	89·2	0	2	1	0	2
36	0·41	3,208·5	2,655·2	127·6	63·8	2	1	1	0	1
37	0·64	14,629·4	12,427·0	191·9	143·9	2	0	1	0	1

- HU, hydrographic unit; R_c, circularity ratio; A_{3D}, tri-dimensional area; A_{2D}, plan area; *L*, length; *MSI*, morphometric slope index; *Ls*, landslides; *G*, gullies; *R*, rills; *P*, pipes.

Table 2. Results of the cluster analysis

Clusters	
1	**2**
59·5% (22)	**40·5% (15)**
G	*G*
No gullies (81·8%)	Gullies prevalence (100%)
Ls	*Ls*
Landslides prevalence (100%)	No landslides (53·3%)
P	*P*
No pipes (86·4%)	Yes pipes (86·7%)
R	*R*
Yes rills (54·5%)	Yes rills (73·3%)

- Each column represents the two clusters in which the 37 HUs were grouped (1 and 2). The first row indicates the size of each cluster, in number of HU and percentage on the total. The other rows indicate the main variable categories with the relative importance, in percentage and in different shades of blue (as reported in Figure 5). The discriminating factors were the absence/prevalence of gullies and the prevalence/absence of landslides (dark blue), followed by pipes (light blue); the least important factor is the presence of rills (slight blue). Cluster 1 was landslides dominated (100%), with secondary associated rills (54·5%) and no gullies (81·8%) and pipes (86·4%); cluster 2 was gullies dominated (100%), strongly associated with co-dominant pipes (86·7%) and rills (73·3%) and no landslides (53·3%).
- *Ls*, landslides; *G*, gullies; *R*, rills; *P*, pipes.

Table 3. Numbers, relative and absolute percentage distribution of each variable categories in the two clusters

	Number		Relative distribution (%)		Absolute distribution (%)	
	Cluster		Cluster		Cluster	
Landforms	**1**	**2**	**1**	**2**	**1**	**2**
No gullies	18	0	81·8	0	48·7	0
Yes gullies	4	0	18·2	0	10·8	0
Gullies prevalence	0	15	0	100	0	40·5
No landslides	0	8	0	53·3	0	21·6
Yes landslides	0	7	0	46·7	0	18·9
Landslides prevalence	22	0	100	0	59·5	0
No pipes	19	2	86·4	13·3	51·4	5·4
Yes pipes	3	13	13·6	86·7	8·1	35·1
No rills	10	4	45·5	26·7	27·0	10·8
Yes rills	12	11	54·5	73·3	32·4	29·8

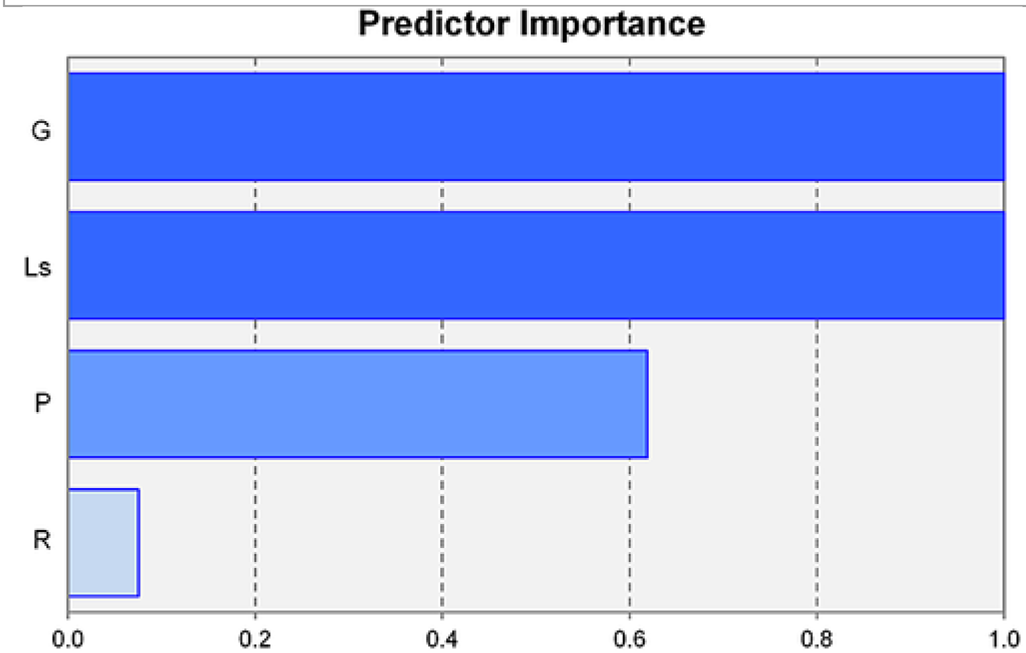

Figure 5
Predictor importance of the erosion variable in the cluster analysis. This figure is available in colour online at wileyonlinelibrary.com/journal/ldr.

The ANOVA, which was carried out to explore the relation between the *MSI* and the cluster partition, showed a significant main effect of the cluster on the values of *MSI* [$F(1, 37) = 4·757$, $p = 0·036$] (Table 4). In particular, the HUs belonging to cluster 1 showed higher *MSI* (Mean = 50·36 m) than the HUs belonging to cluster 2 (Mean = 26·57 m).

Table 4. One-way analysis of variance of morphometric slope index in the two clusters

MSI											
Descriptives						**ANOVA**					
Cluster	***N***	**Mean**	**Std Deviation**	**Minimum**	**Maximum**		**Sum of squares**	***df***	**Mean square**	***F***	**Sig**
1	22	50·36	38·32	15·47	143·93	Between groups	5,048·88	1	5,048·88	4·757	0·036
2	15	26·57	21·22	9·13	89·22	Within groups	37,147·74	35	1,061·36		
Total	37	40·71	34·24	9·13	143·93	Total	42,196·63	36			

- ANOVA, analysis of variance; *MSI*, morphometric slope index.

Discussion

The geomorphological analysis and the detailed field surveys of the Catalfimo area pointed out a great deal of variability of landform typologies and related processes, characterised by variable frequency and intensity. The results of the cluster analysis revealed the relative importance of morphogenetic processes in identifying two groups of HUs: the first was landslides dominated (100%), with secondary associated rills (54·5%) and no gullies and pipes; the second cluster was gullies dominated (100%), strongly associated with co-dominant pipes (86·7%) and rills (73·3%) and no landslides. According to the ANOVA, these two clusters resulted to be controlled by the pre-erosion slope morphometry, as indeed the former had high *MSI* and the latter low *MSI*. This confirmed, through a stochastic approach, that the morphometric characteristics of the HU strongly control their morphodynamic evolution.

These results are completely coherent with specific studies about triggering factors of landslides and gullies. In fact, on clayey terrains, surficial mass movements mostly affect slopes with low to moderate gradient and high contributing area (Zêzere *et al*., 1999; Guzzetti *et al*., 2008; Rotigliano *et al*., 2011, 2012), which correspond to high values of length, width and circularity ratio. Conversely, gullies initiate on steep slopes and low contributing area (Valentin *et al*., 2005; Conoscenti *et al*., 2013, 2014) that corresponds to low length, width and circularity ratio. Moreover, the cluster analysis highlighted the strict connection between surface and subsurface slope processes through the contemporaneous presence or absence of HUs with pipes and gullies in the clusters, confirming that, frequently, gullies formed from the pipe roof collapse (Valentin *et al*., 2005; Faulkner, 2013).

Previous studies demonstrated the validity of *MSI* over common parameters in describing the overall features of the slope, defining the structure of drainage networks and quantifying the rate of soil erosion (Buccolini *et al*., 2012; Buccolini &

Coco, 2013). This study provided a further investigation on the use of this index testing its validity as a general index for slope morphometry and highlighting its influence on the development of different morphogenetic processes. Generally, the combination of morphometric parameters in *MSI* facilitates the study of the relations between morphometry and morphogenesis, avoiding the need to separately analyse the parameters and subsequently to find the relationships between them. Its strength lies in the fact that it combines in a single index a series of parameters, which are usually employed for the morphometric characterisation of drainage systems, making it easy to model and simple to use by specialists and not.

In light of the homogeneity of climatic and geologic conditions of the study area, the results of this research were here interpreted in terms of morphodynamic coupling between the different morphogenetic phenomena, which are responsible for the evolution of the calanchi. However, modifications of the *MSI* values discriminating the two clusters of HUs are to be expected for calanchi areas under different climatic conditions or geologic setting. In this sense, the procedure proposed in this work could be useful for studying and comparing the morphodynamic evolution of other areas of the Apennine, exploiting the *MSI* as a reference morphometric index. *MSI* demonstrated in fact to be as a tool to summarise the different controlling morphometric factors related to the morphogenesis.

Conclusions

A research was carried out in a Sicilian badland area, where calanchi landforms affect clayey slopes. In the area, gully and rill erosion, piping and shallow landslides were recognised as interacting in the shaping of the slopes. The geomorphologic and morphometric characteristics of the HUs in which the study area was partitioned were defined, based on a detailed field survey and a morphometric analysis of a pre-erosion-reconstructed DEM. Depending on the type and the relevance of the different morphogenetic processes, by applying a cluster analysis, two main clusters of HUs were discriminated. Based on the ANOVA, which was performed on the two clusters, the *MSI* morphometric index demonstrated to be relevant in determining the cluster partitioning. In particular, high *MSI* values lead to the absence of gullies and pipes, the prevalence of landslides and the presence of rills; low *MSI* values are responsible for the gullies prevalence, the presence of pipes and rills and the absence of landslides. The results confirmed the importance of the pre-erosion slope morphometry, which was summarised through the *MSI* index, in controlling the morphodynamic behaviour of the HUs in a calanchi area, which is representative of southern Mediterranean Apennine badlands.

Acknowledgements

This study was supported by the University 'G. d'Annunzio' research funding (named Ex-60%) of Professor Marcello Buccolini. The authors would thank the two anonymous reviewers and the editor whose suggestions improved the quality of this paper.

References

Agnesi V, De Cristofaro D, Di Maggio C, Macaluso T, Madonia G, Messana V. 2000. Morphotectonic setting of the Madonie area (central northern Sicily). *Memorie della Societa Geologica Italiana* **55**: 373– 379.

Agnesi V, Camarda M, Conoscenti C, Di Maggio C, Diliberto IS, Madonia P, Rotigliano E. 2005. A multidisciplinary approach to the evaluation of the mechanism that triggered the Cerda landslide (Sicily, Italy). *Geomorphology* **65**: 101– 116. DOI: 10.1016/j.geomorph.2004.08.003

Alexander DE. 1980. I calanchi, accelerated erosion in Italy. *Geography* **65**: 95– 100.

Alexander DE. 1982. Difference between “calanchi” and “biancane” badlands in Italy. In *Badland geomorphology and piping*, RB Bryan, A Yair (eds). edited by Geobooks: Norwich; 71– 88.

Alexander RW, Calvo-Cases A, Arnau-Rosalén E, Mather AE, Lázaro-Suau R. 2008. Erosion and stabilisation sequences in relation to base level changes in the El Cautivo badlands, SE Spain. *Geomorphology* **100**: 83– 90. DOI: 10.1016/j.geomorph.2007.10.025

Aucelli PPC, Conforti M, Della Seta M, Del Monte M, D'Uva L, Rosskopf CM, Vergari F. 2014. Multi-temporal digital photogrammetric analysis for quantitative assessment of soil erosion rates in the Landola catchment of the upper Orcia valley (Tuscany, Italy). *Land Degradation and Development* **In press**. DOI: 10.1002/ldr.2324

Battaglia S, Leoni L, Sartori F. 2003. Mineralogical and grain size composition of clays developing calanchi and biancane erosional landforms. *Geomorphology* **49**: 153– 170. DOI: 10.1016/S0169-555X(02)00171-X

Bouma NA, Imeson AC. 2000. Investigation of relationships between measured field indicators and erosion processes on badland surfaces at Petrer, Spain. *Catena* **40**: 147– 171. DOI: 10.1016/S0341-8162(99)00046-6

Bryan R, Yair A.1982. Perspectives on the studies of badland geomorphology. In *Badland geomorphology and piping*, RB Bryan, A Yair (eds). edited by Geobooks: Norwich; 1– 12.

Buccolini M, Coco L. 2010. The role of the hillside in determining the morphometric characteristics of “calanchi”: the example of Adriatic central Italy. *Geomorphology* **123**: 200– 210. DOI: 10.1016/j.geomorph.2010.06.003

Buccolini M, Coco L. 2013. *MSI* (morphometric slope index) for analyzing activation and evolution of calanchi in Italy. *Geomorphology* **191**: 142– 149. DOI: 10.1016/j.geomorph.2013.02.025

Buccolini M, Gentili B, Materazzi M, Aringoli D, Pambianchi G, Piacentini T. 2007. Human impact and slope dynamics evolutionary trends in the monoclinal relief of Adriatic area of central Italy. *Catena* **71**: 96– 109. DOI: 10.1016/j.catena.2006.07.010

Buccolini M, Coco L, Cappadonia C, Rotigliano E. 2012. Relationships between a new slope morphometric index and calanchi erosion in northern Sicily, Italy. *Geomorphology* **149-150**: 41– 48. DOI: 10.1016/j.geomorph.2012.01.012

Buccolini M, Materazzi M, Aringoli D, Gentili B, Pambianchi G, Scarciglia F. 2014. Late quaternary catchment evolution and erosion rates in the Tyrrhenian side of central Italy. *Geomorphology* **204**: 21– 30. DOI: 10.1016/j.geomorph.2013.07.023

Calzolari C, Ungaro F. 1998. Geomorphic features of a badland (biancane) area (central Italy): characterisation, distribution and quantitative spatial analysis. *Catena* **31**: 237– 256. DOI: 10.1016/S0341-8162(97)00046-5

Campbell IA. 1997. Badlands and badland gullies. In *Arid zone geomorphology: process, form and change in drylands*, (2nd ed.). Wiley: Chichester; 261– 292.

Capolongo D, Pennetta L, Piccarreta M, Fallacara G, Boenzi F. 2008. Spatial and temporal variations in soil erosion and deposition due to land-levelling in a semi-arid area of

Basilicata (southern Italy). *Earth Surface Processes and Landforms* **33**: 364– 379. DOI: 10.1002/esp.1560

Cappadonia C, Conoscenti C, Rotigliano E. 2011. Monitoring of erosion on two calanchi fronts – northern Sicily (Italy). *Landform analysis* **17**: 21– 25.

Caraballo-Arias NA, Conoscenti C, Di Stefano C, Ferro V. 2014. Testing GIS-morphometric analysis of some Sicilian badlands. *Catena* **113**: 370– 376. DOI: 10.1016/j.catena.2013.08.021

Caraballo-Arias NA, Conoscenti C, Di Stefano C, Ferro V. 2015. A new empirical model for estimating calanchi erosion in Sicily, Italy. *Geomorphology* **231**: 292– 300. DOI: 10.1016/j.geomorph.2014.12.017

Castaldi F, Chiocchini U. 2012. Effects of land use changes on badland erosion in clayey drainage basins, Radicofani, central Italy. *Geomorphology* **169-170**: 98– 108. DOI: 10.1016/j.geomorph.2012.04.016

Catalano R, Franchino A, Merlini S, Sulli A. 2000. Central western Sicily structural setting interpreted from seismic reflection profiles. *Memorie della Societa Geologica Italiana* **55**: 5– 16.

Catalano R, Avellone G, Basilone L, Contino A. 2010. Carta Geologica d'Italia 1:50 · 000, Fogli 609 – 596: Termini Imerese – Capo Plaia. http://www.isprambiente.it/MEDIA/carg/596_609_PLAIA_TERMINI/Foglio.html 2010. [Accessed 2014-03-15]

Cerdà A. 1999. Seasonal and spatial variations in infiltration rates in badland surfaces under Mediterranean climatic conditions. *Water Resources Research* **35**: 319– 328. DOI: 10.1029/98WR01659

Cerdà A, García-Fayos P. 1997. The influence of slope angle on sediment, water and seed losses on badland landscapes. *Geomorphology* **18**: 77– 90. DOI: 10.1016/S0169-555X(96)00019-0

Cerdà A, Giménez-Morera A, Bodí MB. 2009. Soil and water losses from new citrus orchards growing on sloped soils in the western Mediterranean basin. *Earth Surface Processes and Landforms* **34**: 1822– 1830. DOI: 10.1002/esp.1889

Ciccacci S, Galiano M, Roma MA, Salvatore MC. 2008. Morphological analysis and erosion rate evaluation in badlands of Radicofani area (southern Tuscany — Italy). *Catena* **74**: 87– 97. DOI: 10.1016/j.catena.2008.03.012

Clarke ML, Rendell HM. 2000. The impact of the farming practice of remodeling hillslope topography on badland morphology and soil erosion processes. *Catena* **40**: 229– 250. DOI: 10.1016/S0341-8162(99)00047-8

Clarke ML, Rendell HM. 2006. Process-form relationships in southern Italian badlands: erosion rates and implications for landform evolution. *Earth Surface Processes and Landforms* **31**: 15– 29. DOI: 10.1002/esp.1226

Clarke ML, Rendell HM. 2010. Climate-driven decrease in erosion in extant Mediterranean badlands. *Earth Surface Processes and Landforms* **35**: 1281– 1288. DOI: 10.1002/esp.1967

Conoscenti C, Agnesi V, Angileri S, Cappadonia C, Rotigliano E, Marker M. 2013. A GIS-based approach for gully erosion susceptibility modelling: a test in Sicily, Italy. *Environmental Earth Sciences* **70**: 1179– 1195. DOI: 10.1007/s12665-012-2205-y

Conoscenti C, Angileri S, Cappadonia C, Rotigliano E, Agnesi V, Marker M. 2014. Gully erosion susceptibility assessment by means of GIS-based logistic regression: a case of Sicily (Italy). *Geomorphology* **204**: 399– 411. DOI: 10.1016/j.geomorph.2013.08.021

Della Seta M, Del Monte M, Fredi P, Lupia Palmieri E. 2007. Direct and indirect evaluation of denudation rates in central Italy. *Catena* **71**: 21– 30. DOI: 10.1016/j.catena.2006.06.008

Della Seta M, Del Monte M, Fredi P, Lupia Palmieri E. 2009. Space-time variability of denudation rates at the catchment and hillslope scales on the Tyrrhenian side of central Italy. *Geomorphology* **107**: 161– 177. DOI: 10.1016/j.geomorph.2008.12.004

Desir G, Marín C. 2013. Role of erosion processes on the morphogenesis of a semiarid badland area. Bardenas Reales (NE Spain). *Catena* **106**: 83– 92. DOI: 10.1016/j.catena.2013.02.011

Dickie JA, Parsons AJ. 2012. Eco-geomorphological processes within grasslands, shrublands and badlands in the semi-arid Karoo, South Africa. *Land Degradation & Development* **23**: 534– 547. DOI: 10.1002/ldr.2170

Erkossa T, Wudneh A, Desalegn B and Taye G. 2015. Linking soil erosion to on-site financial cost: lessons from watersheds in the Blue Nile basin. *Solid Earth* **6**: 765– 774. DOI: 10.5194/se-6-765-2015

Farifteh F, Soeters R. 1999. Factors underlying piping in the Basilicata region, southern Italy. *Geomorphology* **26**: 239– 251. DOI: 10.1016/S0169-555X(98)00070-1

Farifteh J, Soeters R. 2006. Origin of biancane and calanchi in East Aliano, southern Italy. *Geomorphology* **77**: 142– 152. DOI: 10.1016/j.geomorph.2005.12.012

Faulkner H. 2013. Badlands in marl lithologies: a field guide to soil dispersion, subsurface erosion and piping-origin gullies. *Catena* **106**: 42– 53. DOI: 10.1016/j.catena.2012.04.005

Faulkner H, Spivey D, Alexander R. 2000. The role of some site geochemical processes in the development and stabilisation of three badland sites in Almeria, southern Spain. *Geomorphology* **35**: 87– 99. DOI: 10.1016/S0169-555X(00)00024-6

Faulkner H, Alexander R, Zukowskyj P. 2008. Slope–channel coupling between pipes, gullies and tributary channels in the Mocatán catchment badlands, southeast Spain. *Earth Surface Processes and Landforms* **33**: 1242– 1260. DOI: 10.1002/esp.1610

Gabarrón-Galeote MA, Martínez-Murillo JF, Quesada MA, and Ruiz-Sinoga JD. 2013. Seasonal changes in the soil hydrological and erosive response depending on aspect, vegetation type and soil water repellency in different Mediterranean microenvironments. *Solid Earth* **4**: 497–509, DOI: 10.5194/se-4-497-2013, 2013.

Gallart F, Marignani M, Pérez-Gallego N, Santi E, Maccherini S. 2013. Thirty years of studies on badlands, from physical to vegetational approaches. A succinct review. *Catena* **106**: 4– 11. DOI: 10.1016/j.catena.2012.02.008

Guàrdia R, Gallart F, Ninot JM. 2000. Soil seed bank and seedling dynamics in badlands of the upper Llobregat basin (Pyrenees). *Catena* **40**: 189– 202. DOI: 10.1016/S0341-8162(99)00054-5

Gugliotta C. 2012. Inner vs. outer wedge-top depozone “sequences” in the late Miocene (late Tortonian–early Messinian) Sicilian foreland basin system; new data from the

Terravecchia formation of NW Sicily. *Journal of Geodynamics* **55**: 41– 55. DOI: 10.1016/j.jog.2011.11.002

Gugliotta C, Agate M. 2010. Tectonically-enhanced deposition in the late Tortonian Scillato basin (N Sicily): a sequence stratigraphic view. *Rendiconti Online della Società Geologica Italiana* **11**: 733– 734.

Gugliotta C, Gasparo Morticelli M. 2010. Evidences of a polyphasic tectonics in a sedimentary basin developed above an orogenic belt; the Scillato basin study case (N Sicily). *Rendiconti Online della Società Geologica Italiana* **11**: 735– 736.

Gutierrez M, Sancho C, Benito G, Sirvent J, Desir G. 1997. Quantitative study of piping processes in badland areas of the Ebro basin, NE Spain. *Geomorphology* **20**: 237– 253.

Guzzetti F, Ardizzone F, Cardinali M, Galli M, Reichenbach P, Rossi M. 2008. Distribution of landslides in the upper Tiber river basin, central Italy. *Geomorphology* **96**: 105– 122. DOI: 10.1016/j.geomorph.2007.07.015

Howard AD. 1994. Badlands. In *Geomorphology of desert environments*, AD Abrahams, AJ Parsons (eds). Chapman & Hall: London; 213– 242.

Howard AD. 1997. Badlands morphology and evolution: interpretation using a simulation model. *Earth Surface Processes and Landforms* **22**: 211– 227.

Hutchinson MF. 1989. A new procedure for gridding elevation and stream line data with automatic removal of spurious pits. *Journal of Hydrology* **106**: 211– 232. DOI: 10.1016/0022-1694(89)90073-5

Kasanin-Grubin M. 2013. Clay mineralogy as a crucial factor in badland hillslope processes. *Catena* **106**: 54– 67. DOI: 10.1016/j.catena.2012.08.008

Kuhn NJ, Yair A. 2004. Spatial distribution of surface conditions and runoff generation in small arid watersheds, Zin valley badlands, Israel. *Geomorphology* **57**: 183– 200. DOI: 10.1016/S0169-555X(03)00102-8

Lee J-W, Park, C-M, Rhee H. 2013. Revegetation of decomposed granite roadcuts in Korea: developing digger, evaluating cost effectiveness, and determining dimensions of drilling holes, revegetation species, and mulching treatment. *Land Degradation and Development* **24**: 591– 604. DOI: 10.1002/ldr.2248

Lin L, Oguchi T. 2004. Drainage density, slope angle, and relative basin position in Japanese bare lands from high-resolution DEMs. *Geomorphology* **63**: 159– 173. DOI: 10.1016/j.geomorph.2004.03.012

Martínez-Murillo JF, Nadal-Romero E, Regüés D, Cerdà A, Poesen J. 2013. Soil erosion and hydrology of the western Mediterranean badlands throughout rainfall simulation experiments: a review. *Catena* **106**: 101– 112. DOI: 10.1016/j.catena.2012.06.001

Mekonnen M, Keesstra SD, Stroosnijder L, Baartman JEM, Maroulis J. 2015. Soil conservation through sediment trapping: a review. *Land Degradation and Development*, **26**, 544– 556. DOI: 10.1002/ldr.2308.

Mekonnen M, Keesstra SD, Baartman JE, Ritsema CJ, Melesse AM. 2015. Evaluating sediment storage dams: structural off-site sediment trapping measures in northwest Ethiopia. *Cuadernos de Investigación Geográfica* **41**: 7– 22. DOI: 10.18172/cig.2643.

Miller VC. 1953. A quantitative geomorphic study of drainage basin characteristics in clinic mountain area, Virginia and Tennessee. *Project NR 389-042*, *Technical Report* **3**.

Columbia University, Department of Geology, O.N.R. Geography Branch, New York, 1953.

Montgomery DR. 2001. Slope distributions, threshold hillslopes, and steady-state topography. *American Journal of Science* **301**: 432– 454.

Montgomery DR, Dietrich WE. 1994. A physically based model for the topographic control of shallow landsliding. *Water Resources Research* **30**: 1153– 1171.

Moretti S, Rodolfi G. 2000. A typical “calanchi” landscape on the eastern Apennine margin (Atri, central Italy): geomorphological features and evolution. *Catena* **40**: 217– 228. DOI: 10.1016/S0341-8162(99)00086-7.

Nadal-Romero E, Regüés D, Martí-Bono C, and Serrano-Muela P. 2007. Badland dynamics in the central Pyrenees: temporal and spatial patterns of weathering processes. *Earth Surface Processes and Landforms* **32**: 888– 904. DOI: 10.1002/esp.1458.

Nadal-Romero E, Petrlic K, Verachtert E, Bochet E, Poesen J. 2014. Effects of slope angle and aspect on plant cover and species richness in a humid Mediterranean badland. *Earth Surface Processes and Landforms* **39**: 1705– 1716. DOI: 10.1002/esp.3549.

Oguchi T. 1997. Drainage density and relative relief in humid steep mountains with frequent slope failure. *Earth Surface Processes and Landforms* **22**: 107– 120.

Parker RS. 1977. Experimental study of drainage basin evolution and its hydrologic implications. *PhD dissertation*. Colorado State University, Fort Collins.

Pelletier JD. 2003. Drainage basin evolution in the rainfall erosion facility: dependence on initial conditions. *Geomorphology* **53**: 183– 196. DOI: 10.1016/S0169-555X(02)00353-7

Phillips CP. 1998. The badlands of Italy: a vanishing landscape? *Applied Geography* **18**: 243– 257. DOI: 10.1016/S0143-6228(98)00005-8

Pulice I, Cappadonia C, Scarciglia F, Robustelli G, Conoscenti C, De Rose R, Rotigliano E, Agnesi V. 2012. Geomorphological, chemical and physical study of “calanchi” landforms in NW Sicily (southern Italy). *Geomorphology* **153-154**: 219– 231. DOI: 10.1016/j.geomorph.2012.02.026

Regüés D, Gallart F. 2004. Seasonal patterns of runoff and erosion responses to simulated rainfall in a badland area in Mediterranean mountain conditions (Vallcebre, southeastern Pyrenees). *Earth Surface Processes and Landforms* **29**: 755– 767. DOI: 10.1002/esp.1067.

Romero Díaz A, Marín Sanleandro P, Sánchez Soriano A, Belmonte Serrato F, Faulkner H. 2007. The causes of piping in a set of abandoned agricultural terraces in southeast Spain. *Catena* **69**: 282– 293. DOI: 10.1016/j.catena.2006.07.008.

Rotigliano R, Agnesi V, Cappadonia C, Conoscenti C. 2011. The role of the diagnostic areas in the assessment of landslide susceptibility models: a test in the Sicilian chain. *Natural Hazards* **58**: 981– 999. DOI: 10.1007/s11069-010-9708-1

Rotigliano E, Cappadonia C, Conoscenti C, Costanzo D, Agnesi V. 2012. Slope units-based flow susceptibility model: using validation tests to select controlling factors. *Natural Hazards* **61**: 143– 153. DOI: 10.1007/s11069-011-9846-0.

Schumm SA. 1956. Evolution of drainage systems and slopes in badlands at Perth Amboy, New Jersey. *Bulletin of the Geological Society of America* **67**: 597– 646.

Schumm SA, Mosley MP, Weaver WE. 1987. *Experimental fluvial geomorphology*. Wiley-Interscience: New York.

Seutloali KE, Beckedahl HR. 2015. Understanding the factors influencing rill erosion on roadcuts in the south eastern region of South Africa. *Solid Earth* **6**: 633– 641. DOI: 10.5194/se-6-633-2015.

Sirvent J, Desir G, Gutierrez M, Sancho C, Benito G. 1997. Erosion rates in badland areas recorded by collectors, erosion pins and profilometer techniques (Ebro Basin, NE-Spain). *Geomorphology* **18**: 61– 75.

Solé A, Calvo A, Cerdà A, Lázaro R, Pini R, Barbero J. 1997. Influences of micro-relief patterns and plant cover on runoff related processes in badlands from Tabernas (SE Spain). *Catena* **31**: 23– 38. DOI: 10.1016/S0341-8162(97)00032-5.

Talling PJ, Sowter MJ. 1999. Drainage density on progressively tilted surfaces with different gradients, Wheeler Ridge, California. *Earth Surface Processes and Landforms* **24**: 809– 824. DOI: 10.1002/(SICI)1096-9837(199908)24:9<809::AID-ESP13>3.0.CO;2-R

Torri D, Bryan R. 1997. Micropiping processes and biancana evolution in southeast Tuscany. *Geomorphology* **20**: 219– 235.

Torri D, Santi E, Marignani M, Rossi M, Borselli L, Maccherini S. 2013. The recurring cycles of biancana badlands: erosion, vegetation and human impact. *Catena* **106**: 22– 30. DOI: 10.1016/j.catena.2012.07.001.

Tucker GE, Bras RL. 1998. Hillslope processes, drainage density, and landscape morphology. *Water Resources Research* **34**: 2751– 2764.

Valentin C, Poesen J, Li Y. 2005. Gully erosion: impacts, factors and control. *Catena* **63**: 132– 153. DOI: 10.1016/j.catena.2005.06.001.

Vergari F, Della Seta M, Del Monte M, Fredi P, Lupia Palmieri E. 2013. Long- and short-term evolution of several Mediterranean denudation hot spots: the role of rainfall variations and human impact. *Geomorphology* **183**: 14– 27. DOI: 10.1016/j.geomorph.2012.08.002.

Vericat D, Smith MW, Brasington J. 2014. Patterns of topographic change in sub-humid badlands determined by high resolution multi-temporal topographic surveys. *Catena* **120**: 164– 176. DOI: 10.1016/j.catena.2014.04.012.

Vittorini S. 1977. Osservazioni sull'origine e sul ruolo di due forme di erosione nelle argille: calanchi e biancane. *Bollettino della Società Geografica Italiana* **6**: 25– 54.

Yair A, Bryan RB, Lavee H, Schwanghart W, Kuhn NJ. 2013. The resilience of a badland area to climate change in an arid environment. *Catena* **106**: 12– 21. DOI: 10.1016/j.catena.2012.04.006.

Zêzere JL, Ferreira AB, Rodrigues ML. 1999. Landslides in the north of Lisbon region (Portugal): conditioning and triggering factors. *Physics and Chemistry of the Earth* **24**: 925– 934. DOI: 10.1016/S1464-1895(99)00137-4.

Zhao G, Mu X, Wen Z, Wang F, Gao P. 2013. Soil erosion, conservation, and eco-environment changes in the loess plateau of China. *Land Degradation and Development* **24**: 499– 510. DOI: 10.1002/ldr.2246.